32. Absorption Spectra and Termination Kinetics of Transient Free Radicals in Solution Observed by UV./VIS. Spectroscopy with Modulated Excitation

by **Christian Huggenberger** and **Hanns Fischer**

Physikalisch-Chemisches Institut der Universität Zürich, Winterthurerstrasse 190, CH-8057 Zürich

(5.IX.80)

Summary

Free radicals are generated in liquid solutions by harmonically modulated photolysis of suitable substrates. Harmonic analysis of the absorbance as functions of wavelength and modulation frequency yields the optical spectra and the decay kinetics of the transient species. The experimental technique and the analysis are described in detail. Results on *t*-butyl, 2-propyl and benzyl radicals generated by photolysis of the corresponding dialkyl resp. dibenzyl ketones are reported. They confirm previous spectral assignments and show that the termination reactions are diffusion controlled.

1. Introduction. – To supplement our time resolved electron spin resonance (ESR.) investigations of the kinetics of free radical reactions in solution [1] we have now developed a method to study these species and their reactions by optical spectroscopy. For the optical detection of radicals the time resolved techniques of pulse radiolysis [2] and flash photolysis [3] have often been applied. Here, we use an alternative in the variant of harmonic radical generation. The principles rest on the pioneering work of *Hunziker* [5] who has applied the technique to study free radicals in the gas phase, and on the extensions of *Günthard* [6] and *Paul* [7] to liquid phase ESR. investigations.

Free radicals are generated by UV.-photolysis of suitable substrates with light intensities varying sinusoidally in time. Simultaneously, the absorbance of the solution is observed and analyzed by phase sensitive detection on the light modulation frequency. Substrates, transient intermediates and products contribute to the modulated absorbance with amplitudes and phases depending differently on the modulation frequency. Analysis of these dependencies yield the kinetic information. Spectra are obtained from the wavelength dependence of the modulated absorbance at constant frequency.

Compared to other modulation schemes [8] [9] the harmonic variant offers the advantage of simpler data analysis, in particular for the case of second order radical reaction kinetics [5a] [7]. Our version allows the direct and continuous

0018-019X/81/1/0338-16$01.00/0

recording of optical spectra of transient species, a convenience which is not readily obtainable in time resolved techniques.

This paper describes the experimental arrangement and the data analysis in detail. Further, we report optical spectra of *t*-butyl, 2-propyl and benzyl radicals observed during photolysis of the corresponding ketones in liquid solution and rate constants for the bimolecular self-termination of these radicals. In this context a new experimental technique for determining the rate of radical formation from the modulated reactant absorbance is introduced. The results support previous spectral assignments and confirm earlier conclusions on the factors controlling self-termination rate constants of sterically unhindered transient radicals in solution.

2. Experimental Part. – *Figure 1* shows a block diagram of the arrangement. The light of a 1 kW-Hg/Xe-short arc lamp *(Hanovia 977 B-1)*, driven by a stabilized power supply *(Heinzinger TNX 977-B1)*, is transmitted by a suprasil lens to the rectangular reaction cell within the *Dewar* D. The wavelength region of this photolysis beam is limited to $225 \leqq \lambda \leqq 340$ nm by an aqueous Ni/Co-sulfate-solution filter F and can be narrowed further by additional glass filters *(Schott)*. Harmonic modulation of the light intensity in the reaction cell is achieved *via* sine-diaphragms [7]: The *suprasil* lens forms an enlarged image of the Hg/Xe arc in the center plane of the cell, which is positioned in a homogeneous section of this image. Directly after and as close as possible to the lens the light passes through a modulator M which consists of specially formed stationary slots and the rotating sector disk (on-off period 1:1) of a light chopper *(Ortec Brookdeal 9479)*. Since slots and sector disk are positioned close to the principal plane of the lens the light intensity at the sample varies proportionally to the open fraction of the slot area. This area is shaped in such a way that a sector edge traversing it with constant angular velocity causes a sinusoidal variation of the open fraction. Two different slot arrangements are displayed in *Figure 2*. The arrangement with three small slots ensures a good harmonicity and was used in all kinetic runs. The larger sine-diaphragm allows an increased photolysis intensity and was used for recording radical spectra. With the original chopper the modulation frequency could be varied in the range $10 \leqq \nu \leqq 1000\ s^{-1}$. For frequencies in the range $0.5 \leqq \nu \leqq 10\ s^{-1}$ an external sector drive was installed.

The absorbance of the sample is detected by the analyzing light beam at right angle to the photolysis beam. It consists of a Xe high pressure lamp *(Osram XBO 450W)* driven by a power supply *(Heinzinger TNX 450)* and passes the sample nearly parallel before entering the grating monochromator GM (blaze 300 nm, linear dispersion 2 nm/mm, aperture ratio 1:8). Glass filters F eliminate light of unwanted wavelengths. A large distance between reaction cell and monochromator ensures that modulated stray light of the photolysis beam or sample luminescence do not contribute significantly to the signal of the photomultiplier PM (*Hamamatsu R 955*, driven with 5 dynodes).

In the electronic circuitry the photomultiplier signal is fed into the signal channel of a heterodyne lock-in-amplifier PSD (*Ortholoc-SC 9505* in sinetrac response mode, or *Ithaco Dynatrac 391 A*) either

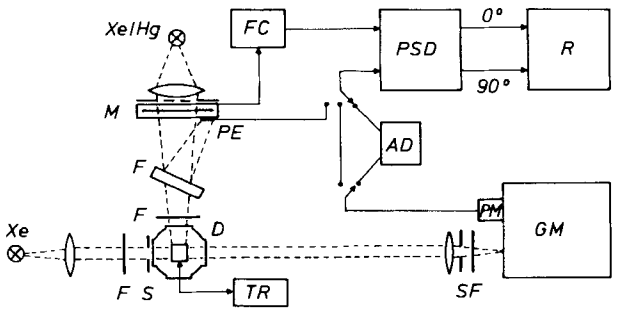

Fig. 1. *Block diagram.* For abbreviations see text.

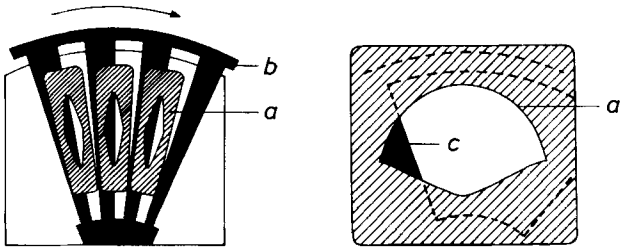

Fig. 2. *Light-modulator arrangement.* Left: Three-slot version with a) diaphragm, b) sector disk. Right: One-slot version with a) diaphragm, c) leading edge of sector blade.

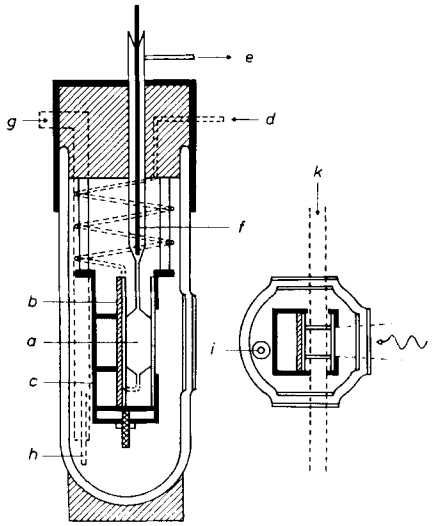

Fig. 3. *Sample arrangement.* For abbreviations see text.

directly or *via* an AC/DC analog voltage divider AD. The reference signal is taken from the light-chopper. It is measured in a counter FC *(Iwatsu FC-8841)*. The output of the lock-in-amplifier, *i.e.* the phase-sensitively detected in-phase, out-of-phase or amplitude signals on the modulation frequency is directly recorded (R = *Rikadenki R-22* or *Servogor RE 541*). Weak and noisy signals can be time-averaged by an analog integrator.

For exact phase adjustments of the PSD a reference signal is derived from the photolysis beam by reflecting a small part of the light at the surface of the cuvette containing the filter solution to a photodiode *(AEG)* mounted in an image of the arc (PE).

Figure 3 shows the sample cell arrangement. The reaction cell *a* is a 5×5 mm^2 rectangular micro-flow-cuvette *(Starna Type 43)*, 10 mm long, fixed by a suitable holder *c* within a quartz *Dewar* with fused plane suprasil windows. A mirror *b (Alflex Balzers)* on the backside of the cell reflects the not absorbed part of the photolysis light to improve the homogeneity and to increase the intensity of the photolysis light in the cell. The sample solution flows continuously from a motor-driven syringe through the cell *via* a stainless steel capillary spiral located within the *Dewar* (entrance port *d*, outlet *e*, flow rates typically 0.5–1 ml/min). For the temperature adjustment precooled gaseous nitrogen is pumped into the *Dewar* (entrance port *g*) and heated electrically to the desired temperature range (heater and sensor *h, i*). The sample temperature is measured in the outgoing solution by a thermocouple *f*. The detecting beam *k* probes the center portion of the cell over an area of 4.5×3 mm^2.

The distribution of the modulated photolysis light was measured at the position of the sample cell by replacing the sample by a UV.-sensitive detector [10] shielded by a small hole diaphragm. For the three-slot-modulator *(Fig. 2)* the phase accuracy was within $\pm 0.5°$ and the content of higher harmonics $(\sum_{n>1} J^2_{n\omega})^{1/2}/J_\omega$ was $\leq 3\%$ over the whole sample cell and for all modulation frequencies. The same arrangement served to check the phase adjustment procedure described above.

Di-*t*-butylketone, diisopropylketone and dibenzylketone were purchased in the purest available qualities *(Fluka, Merck)*. Dibenzylketone was recrystallized from hexane. 3-Methyl-3-pentanol *(Koch-Light)* was freshly distilled before use, hexadecane *(Koch-Light)* was purified by column chromatography. Cyclohexane *(Merck)* was used in spectroscopically pure quality. All solutions were deoxygenated by purging with helium.

Absorption spectra of free radicals were obtained at fixed modulation frequencies with the one-slot modulator and broad-band photolysis using the analog voltage divider. Solution flow rates were typically 1 ml/min. The spectra were recorded directly (amplitude) with monochromator scan rates of about 20 nm/min, a time constant of 1 s and resolutions of 1–2 nm. In kinetic runs, the three-slot modulator was applied and special care was taken to ensure homogeneous conditions in the reaction cell: The excitation region was limited to the longest wavelength absorption band of the ketone, the substrate concentration was selected to correspond to less than 10% absorption at 313 nm. With flow rates of typically 0.5 ml/min the conversion of the ketone in the cell was usually less than 10%. Further, the frequency dependencies of amplitudes, in-phase and out-of-phase components were measured without use of the voltage divider since this was found to cause a frequency dependent phase shift. To obtain the DC-voltage this was determined independently at the working resistor of the photomultiplier. The applied substrate concentrations are given later together with experimental results.

3. Analysis. – The modulated photolysis leads to a modulation of the absorbance of the sample. If D_- is the DC- and $D_\sim$ the AC-component of the sample's optical density, *Lambert-Beer*'s law for the intensity of the detecting beam can be written as

$$J = J_- + J_\sim = J_0 \exp\{-\ln 10\,(D_- + D_\sim)\}. \tag{1}$$

For $|D_\sim| \ll 1$ this becomes

$$J = J_- + J_\sim = J_-\{1 - \ln 10 \cdot D_\sim\}. \tag{2}$$

The photomultiplier voltage is proportional to J, and, accordingly, contains DC- and AC-components V_- and $V_\sim$. For the ratio, equ. 2 leads to

$$\frac{V_\sim}{V_-} = \frac{J - J_-}{J_-} = -\ln 10 \cdot D_\sim. \tag{3}$$

A voltage which is proportional to this ratio is provided by the AC/DC divider in the experimental arrangement. The lock-in-amplifier determines amplitude and phase of the first harmonic contribution to this voltage or to $V_\sim$ directly, if V_- is measured separately. Correspondingly, $D_\sim$ is obtained after correction for the proportionality constants from the lock-in-amplifier signal as amplitude ΔD and phase φ of the first harmonic contribution

$$D^1_\sim = \Delta D \cos(\omega t + \varphi). \tag{4}$$

If several chemical species X contribute to D one has

$$D^1_{\sim} = \sum_X \Delta D_X \cos(\omega t + \varphi_X) \tag{5}$$

with

$$\Delta D_X = \varepsilon_X \cdot l \cdot \Delta [X] \tag{6}$$

where ε_X denotes the decadic extinction coefficient of species X, $\Delta [X]$ the modulation amplitude of its concentration and l the optical path length along the detection axis.

All chemical systems treated in this work obey a simple reaction scheme:

$$E \xrightarrow{1} 2R \tag{7}$$

$$2R \xrightarrow{k} P$$

where

$$I = \frac{I_o}{2}(1 + \cos\omega t) \tag{8}$$

is the rate of formation of radicals R from the substrates E, and k is the self-termination rate constant. P denotes the radical reaction products.

The kinetic equations for the concentrations of the various species within the sample subvolume probed by the detection beam are then

$$-\frac{d[E]}{dt} = \frac{1}{2} I - \frac{1}{\tau}([E]_i - [E]_o) \tag{9}$$

$$\frac{d[R]}{dt} = I - 2k[R]^2 + \frac{1}{\tau}([R]_i - [R]_o) \tag{10}$$

$$\frac{d[P]}{dt} = k[R]^2 + \frac{1}{\tau}([P]_i - [P]_o). \tag{11}$$

The last terms on the right hand sides of eqs. 9-11 account for the flow of the solutions. τ is the dwell time in the zone of observation, and the lower indices i and o denote the in- and out-going fluxes. For a continuous flow all concentrations will be composed of time independent average terms and modulated components

$$[X] = \overline{[X]} + [X]_{\sim}. \tag{12}$$

The dwell time τ is of the order of 20 s and large if compared to both radical lifetime ($\sim 10^{-3}$ s) and inverse modulation frequency. Therefore, we may neglect

flow terms in equ. 10 and their contributions to the modulation of [E] and [P]. This leads to simplified equations for the time-dependent terms

$$-\frac{d[E]_\sim}{dt} = \frac{I_o}{4}\cos\omega t \tag{13}$$

$$\frac{d[R]_\sim}{dt} = \frac{I_o}{2}\cos\omega t - 2k(2\overline{[R]}\cdot[R]_\sim + [R]_\sim^2) \tag{14}$$

$$\frac{d[P]_\sim}{dt} = k(2\overline{[R]}\cdot[R]_\sim + [R]_\sim^2) \tag{15}$$

and to

$$\overline{[R]} = (I_o/4k)^{1/2}\,. \tag{16}$$

Integration of equ. 13 shows $[E]_\sim$ to be of the form

$$[E]_\sim = \Delta[E]\cdot\cos(\omega t + \varphi_E) \tag{17}$$

with

$$\Delta[E] = \frac{I_o}{4\omega} \tag{18}$$

$$\varphi_E = \pi/2\,. \tag{19}$$

Approximate solutions of equ. 14 may be obtained with the Ansatz

$$[R]_\sim = \Delta[R]\cdot\cos(\omega t + \varphi_R) \tag{20}$$

and $\Delta[R] \ll \overline{[R]}$, and gives

$$\Delta[R] = \frac{1}{2} I_o(\omega^2 + \tau_R^{-2})^{-1/2} \tag{21}$$

$$\mathrm{tg}\,\varphi_R = -\omega\tau_R \tag{22}$$

with τ_R, the radical lifetime, defined as

$$\tau_R = (4k I_o)^{-1/2} \tag{23}$$

As *Hunziker* [5] and *Paul* [7] have shown the eqs. 20–22 agree very closely with the exact solutions of equ. 14 for $\omega\tau_R \geqq 1$ and do not deviate strongly from these for the whole frequency range.

From equ. 15, $[R]_{\sim} \ll \overline{[R]}$, and eqs. 20–22 we obtain finally for the product

$$[P]_{\sim} = \Delta[P] \cdot \cos(\omega t + \varphi_P) \tag{24}$$

$$\Delta[P] = \frac{I_o}{4\omega\tau_R} (\omega^2 + \tau_R^{-2})^{-1/2} \tag{25}$$

$$\varphi_P = \varphi_R - \pi/2 . \tag{26}$$

Figures 4 and *5* show the frequency dependencies of amplitudes $\Delta[X]$ and phases φ_X for reactant, radical and product. Obviously, the modulated reactant concentration can be detected most easily at low frequencies, and the contributions of all three species to $D_{\sim}$ (equ. 5) can be separated by appropriate phase and frequency selection.

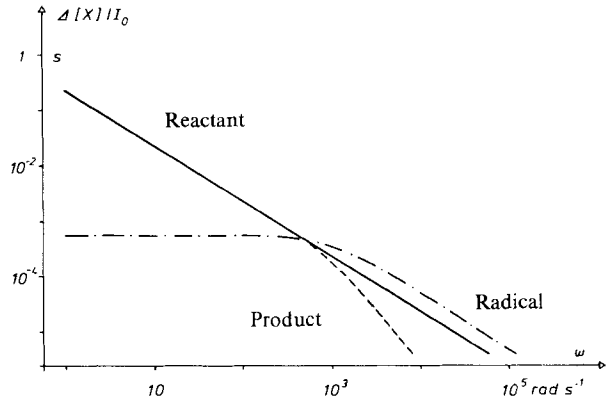

Fig. 4. *Frequency dependencies of spectral amplitudes for* $\tau_R = 10^{-3}$ *s.*

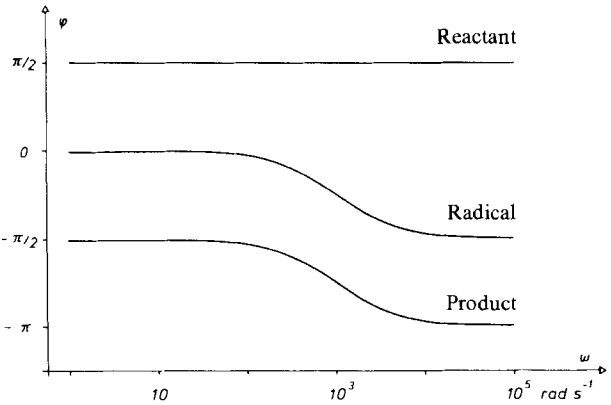

Fig. 5. *Frequency dependencies of phases for* $\tau_R = 10^{-3}$ *s.*

As suggested by the above analysis we will subsequently detect free radicals under the condition $\omega\tau_R \geqq 1$ and in spectral regions where educt and products do not contribute significantly to $D_\sim$. As eqs. 5, 6 and 21 show, a plot of $(\Delta D)^{-2}$ versus ω^2 will then lead to a straight line with slope

$$a_R = 4(\varepsilon_R \cdot l \cdot I_o)^{-2} \tag{27}$$

and ordinate

$$b_R = 4(\varepsilon_R \cdot l \cdot I_o \cdot \tau_R)^{-2} \tag{28}$$

from which the radical lifetime τ_R and the quantity $\varepsilon_R \cdot I_o$ can be determined. Alternatively, τ_R may also be obtained *via* equ. 22 from a plot of the ratio of out-of-phase and in-phase signals, *i.e.* $\mathrm{tg}\varphi_R$ *versus* the modulation frequency.

To determine the termination rate constant k from τ_R *via* equ. 23 and the extinction coefficient ε_R from $\varepsilon_R \cdot I_o$ the rate of radical formation I_o must be known. This quantity can be determined most conveniently from the signal of the reactant absorption at low modulation frequencies (see equ. 18, *Fig. 4* and *5*) if a wavelength region is found where radicals or products have not too large extinction coefficients. Then a comparison of the out-of-phase spectrum with the known reactant spectrum should confirm its identity, and a plot of ΔD *versus* ω^{-1} should yield a line with slope

$$a_E = \frac{1}{4}\varepsilon_E \cdot l \cdot I_o \,. \tag{29}$$

This procedure will be used in the following (to our knowledge it has not yet been applied before).

I_o may also be obtained by observing the decay of the radical signal during modulated photolysis after interrupt of the substrate flow [9a]: For low absorbance of the photolysis light the average reactant concentration will decay exponentially

$$\frac{d\overline{[E]}}{dt} = -\tau_s^{-1}\overline{[E]} \tag{30}$$

with a decay time τ_s. Consequently, the average rate of radical formation becomes time dependent

$$\frac{1}{2} I_o(t) = -2\frac{d\overline{[E]}}{dt} = 2\tau_s^{-1}\overline{[E]}_o \exp(-t/\tau_s) \tag{31}$$

where $\overline{[E]}_o$ denotes the average reactant concentration before the stop of the flow. We will observed the radical signal at very high modulation frequencies $\omega\tau_R \gg 1$ for which eqs. 6, 21 and 31 lead to

$$\Delta D(t) = \frac{2 \cdot \varepsilon_R \cdot l}{\omega} \tau_s^{-1} \cdot \overline{[E]}_o \exp(-t/\tau_s) \tag{32}$$

i.e. an exponential decrease from which τ_s is obtained. Insertion into the expression

$$I_o = 4\,\tau_s^{-1}\,\overline{[E]}_o \tag{33}$$

valid for continuous flow, yields I_o if $\overline{[E]}_o$ is known. This may be obtained from the initial substrate concentration c_o *via*

$$\overline{[E]}_o = \frac{c_o}{z_2 - z_1} \int_{z_1}^{z_2} \exp\left(-\frac{z}{v \cdot \tau_s}\right) dz \tag{34}$$

where v is the flow velocity along the long axis z of the sample cell and z_1 and z_2 are the limits of the observation zone.

4. Results. – 4.1. t-*Butyl radical.* The radicals were generated by photolysis of di-*t*-butylketone *via* the following reaction sequence [1a, b] [11] [12]:

$$(CH_3)_3CCOC(CH_3)_3 \xrightarrow{h\nu} (CH_3)_3C\dot{C}O + \dot{C}(CH_3)_3$$

$$(CH_3)_3C\dot{C}O \longrightarrow (CH_3)_3\dot{C} + CO$$

$$2\,(CH_3)_3\dot{C} \longrightarrow (CH_3)_3CH + (CH_3)_2C{=}CH_2$$

$$2\,(CH_3)_3\dot{C} \longrightarrow (CH_3)_3C{-}C(CH_3)_3.$$

At room temperature and above radical formation from the excited state precursors and the decarbonylation of the pivaloyl radical are very rapid if compared to the radical termination rates [11] [12a]. Consequently, apart from a very small cage fraction [12b] all products arise from the reactions given above. Further, any phase shifts arising from finite radical formation rates can be neglected, *t*-butyl

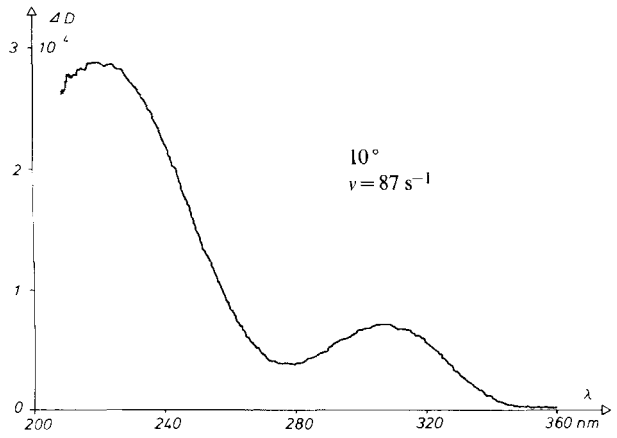

Fig. 6. *Absorption spectrum of* t-*butyl radicals in 3-methyl-3-pentanol.*

should be the only observable radical, and the system conforms according to equ. 7.

Figure 6 shows an absorption spectrum observed during photolysis of di-*t*-butylketone 0.023 M in 3-methyl-3-pentanol at 10° with a modulation frequency $\nu = 87\ s^{-1}$ (resolution 2 nm). The 'shape' of the spectrum did not depend on the photolysis intensity, solvent (3-methyl-3-pentanol, cyclohexane or methanol), temperature (10, 30°), and modulation frequency (70, 87 or 214 s^{-1}). Amplitude and phases of the two bands at 220 and 307 nm showed equal dependencies on the modulation frequencies, and they were those expected for free radicals *(vide infra)*. Therefore, we attribute the spectrum to *t*-butyl. Contributions of pivaloyl are deemed unlikely, also in view of the short lifetime of this species and the known spectral characteristics of acyl radicals [1d].

As far as we know the absorption spectrum of *t*-butyl in liquid solution has not yet been reported. In the gas-phase *Parkes & Quinn* have observed the spectrum in the region $210 \leqq \lambda \leqq 280$ nm [9b, c]. It consists of a broad band extending from 220 to 240 nm with a maximum at 229 nm ($\sigma = 5 \cdot 10^{-18}$ cm^2 [9b], $8 \cdot 10^{-18}$ cm^2

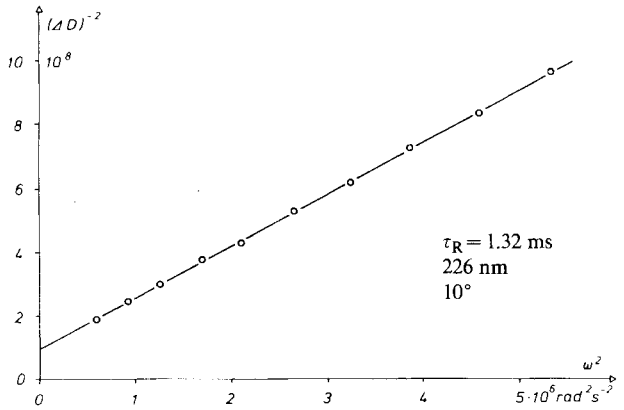

Fig. 7. *Frequency dependence of ΔD for* t-*butyl in 3-methyl-3-pentanol.*

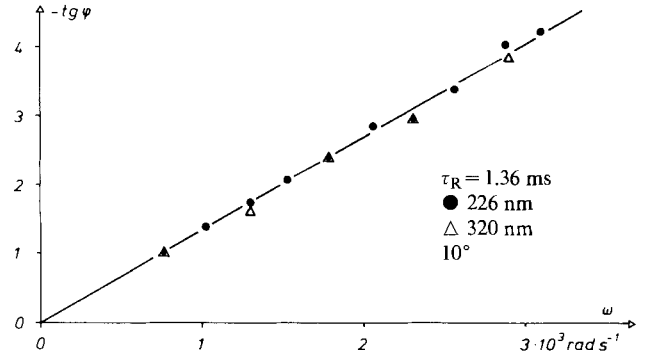

Fig. 8. *Frequency dependence of φ for* t-*butyl in 3-methyl-3-pentanol*

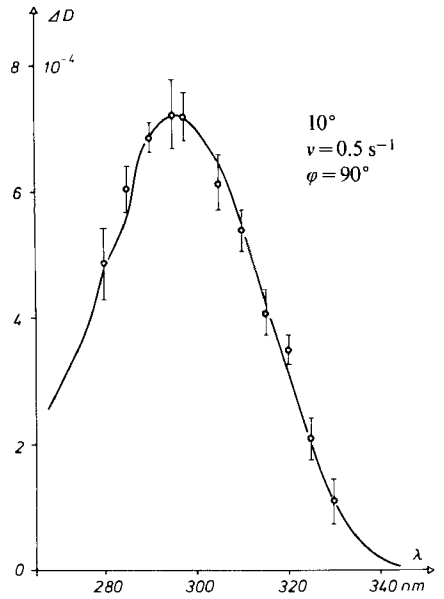

Fig. 9. *Effect spectrum at low modulation frequency.* Solid line: $n\pi^*$-absorption band of di-*t*-butylketone.

[9c]) and a shoulder extending to 270 nm. Our spectrum roughly agrees with their findings for $\lambda \leqq 280$ nm. In addition we find weaker band at 307 nm, *i.e.* at astonishingly long wavelengths.

Figures 7 and *8* show the frequency dependencies of the signal amplitudes ΔD and phases φ of *t*-butyl at the two absorption maxima as obtained with 0.0188 M ketone solutions in 3-methyl-3-pentanol at 10°. The straight lines are excellent confirmations of the conclusions of the analysis section. Further, within the error limits the radical lifetimes τ_R obtained from both plots are nearly identical.

Figure 9 displays an effect spectrum taken point by point during photolysis of a 0.056 M solution of di-*t*-butylketone in 3-methyl-3-pentanol with the very low modulation frequency of 0.5 s^{-1} and the phase-angle set to $\varphi = \pi/2$. The curve drawn in the *Figure* is the $n\pi^*$-absorption band of the ketone. Obviously, the modulated signal has to be ascribed to the reactant. *Figure 10* shows the frequency dependence of its amplitude at the absorption maximum taken with a 0.0188 M solution. As expected, equ. 18 is fulfilled. From the slope of the straight line and ε_E (297) = 21.2 $M^{-1} \cdot cm^{-1}$ the rate of radical formation I_o is obtained *via* equ. 29. This is then used to evaluate the rate constant of radical termination and the extinction coefficient of the radical from the parameters obtained from *Figures 7* and *8* (eqs. 22, 27 and 28).

The rate of radical formation was also obtained from the decrease of the radical signal after stopping the flow of the solution. *Figure 11* displays the exponential decay corresponding to equ. 32. The value of $I_o = 3.6 \cdot 10^{-4}$ M $\cdot s^{-1}$ obtained from τ_s agrees well with that resulting from the plot of *Figure 10* ($4.0 \cdot 10^{-4}$ M $\cdot s^{-1}$). Insertion of I_o as given in *Figure 10* into equ. 27 leads with

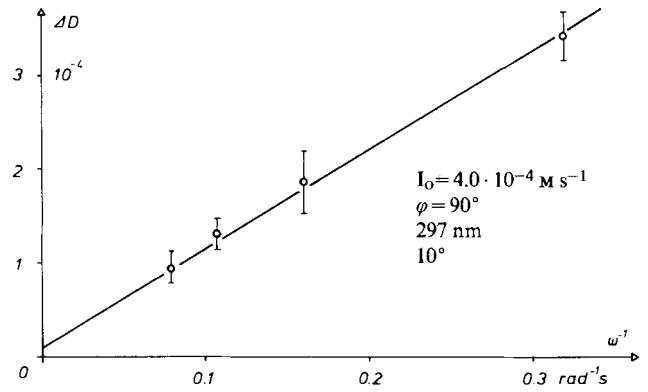

Fig. 10. *Frequency dependence of ΔD at low modulation frequencies and I_0 for* t-*butyl*

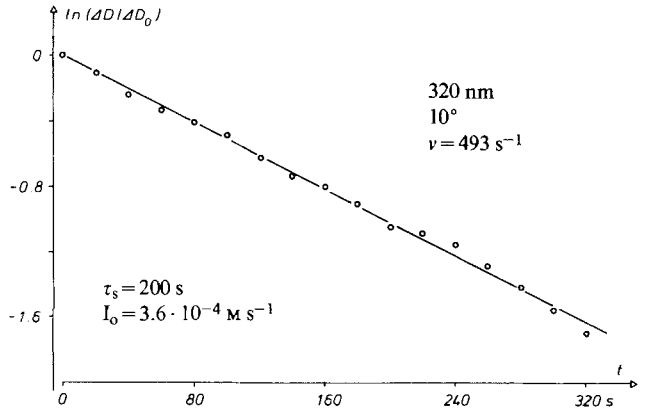

Fig. 11. *Determination of I_0 for* t-*butyl from τ_s*

the values of a_R from plots of the type of *Figure 7* to the extinction coefficients of *t*-butyl of $\varepsilon_R = (800 \pm 40)$ M^{-1} · cm^{-1} at $\lambda = 220$ nm and $\varepsilon_R = (200 \pm 20)$ M^{-1} · cm^{-1} at $\lambda = 307$ nm. *Parkes & Quinn* stated $\varepsilon_R =$ 1300 M^{-1} cm^{-1} [9b] and $\varepsilon_R = 2100$ M^{-1} · cm^{-1} [9c] at 229 nm. These values are compatible with though somewhat higher than our data. All results of this section are also listed in the *Table,* and the kinetic constants will be discussed subsequently.

4.2. *2-Propyl radical.* Photolysis of diisopropylketone leads to the formation of 2-propyl radicals in a reaction sequence analogeous to that given above for di-*t*-butylketone [13–15]. For $T \geqq 30°$ decarbonylation of the isobutyryl radical is fast compared to all radical terminations, *i.e.* the system conforms according to the simplified scheme of equ. 7. An absorption spectrum taken at intermediate modulation frequency during photolysis of the ketone 0.033 M in hexadecane at 38° is given in *Figure 12* (resolution 2 nm). Amplitude and phase show the frequency dependence expected for a free radical intermediate, see below, and we ascribe the spectrum to 2-propyl for this reason. The gas-phase work of

Table. *Spectral features and termination rate constants of transient radicals in liquid solutions*

Radical	T [°C]	λ_{max} [nm]	ε_{max} [M^{-1} cm^{-1}]	$2k$ [10^9 M^{-1} s^{-1}]	$^{2k}/_{2k^{th}}$
t-Butyl in 3-methyl-3-pentanol	10	220	800 ± 40	0.71 ± 0.06	0.93
		307	200 ± 20		
2-Propyl in hexadecane	39	220	1,000 ± 50	3.5 ± 0.4	1.14
Benzyl in cyclohexane	24	258	31,400 ± 3,200	3.6 ± 0.2	1.03
		293	1,400 ± 200		
		304	3,500 ± 400		
		316	8,800 ± 700		
		422	95 ± 20		
		436	120 ± 20		
		452	130 ± 20		

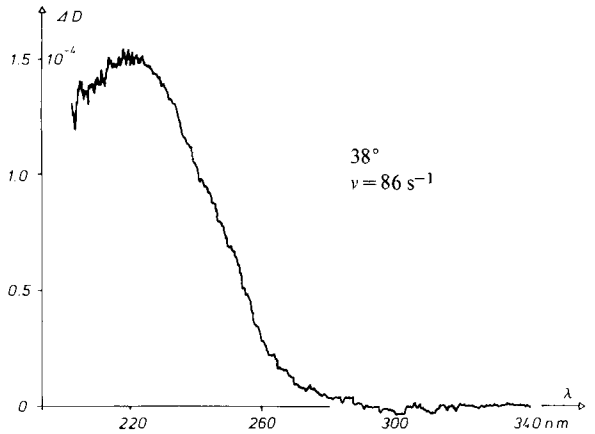

Fig. 12. *Absorption spectrum of 2-propyl radicals in hexadecane*

Parkes & Quinn [9c] has revealed a broad absorption with a maximum at 233 nm. We find in solution a similar structureless band with onset at 290 nm and maximum at 220 nm. The radical lifetime τ_R and $\varepsilon_R \cdot I_0$ were determined with 0.0254 M ketone solutions at 39° from the frequency dependencies of ΔD and φ at $\lambda = 220$ nm. Both methods lead to $\tau_R = (0.78 \pm 0.01)$ ms. For the determination of I_0 an effect spectrum was taken with a 0.029 M ketone solution at 38° and a low modulation frequency of 0.5 s^{-1}. It agreed with the $n\pi^*$-absorption band of the ketone, and the frequency dependence of its out-of-phase component obtained at $\lambda = 290$ nm with the 0.0254 M ketone solution lead with $\varepsilon_E(290) = 25.6$ $M^{-1} \cdot cm^{-1}$ to $I_0 = 2.3 \cdot 10^{-4}$ $M \cdot s^{-1}$. As in section 4.1, I_0 was also determined from the decay time τ_s of the radical absorption after a stop of the flow at a high modulation frequency (660 s^{-1}). The result ($I_0 = 2.1 \cdot 10^{-4}$ $M \cdot s^{-1}$) agrees with that obtained from the reactant spectrum. From $\varepsilon_R \cdot I_0$ and I_0 the radical extinction coefficient is $\varepsilon_R(220) = (1000 \pm 50)$ $M^{-1} \cdot cm^{-1}$. This value agrees with the previous gas-phase data of $\varepsilon_R(233) = 1000$ $M^{-1} \cdot cm^{-1}$ and 920 $M^{-1} \cdot cm^{-1}$ [9c] [16]. The termination rate constant obtained from τ_R and I_0 is given in the *Table* and will be discussed later.

4.3. *Benzyl radical.* The photolysis of dibenzylketone provides a clean source of benzyl radicals *via* the following reaction scheme [1c] [13] [17]:

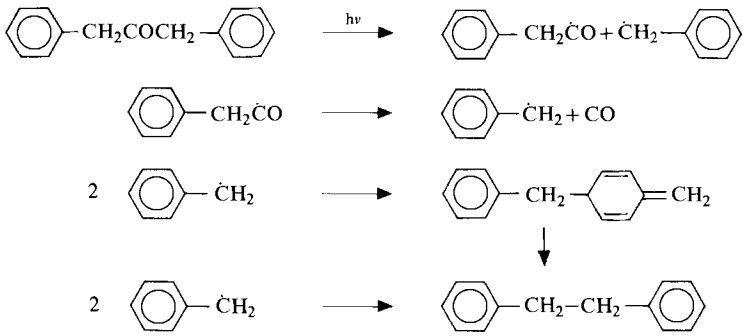

Again, at room temperature and above the decarbonylation of the acyl radical is fast if compared with the termination reactions. The benzyl radicals lead to bibenzyl in nearly quantitative yields, in part *via* isomerization of unstable semibenzenes which result from αo- and αp-coupling. These can be converted to benzylsubstituted toluenes by addition of acids [17].

Figure 13 shows an absorption spectrum taken with $v = 91\ s^{-1}$ during photolysis of dibenzylketone 0.0023 M in cyclohexane at 24° (resolution 1 nm). It is attributed to benzyl radicals. Contributions of the semibenzenes are excluded, since solutions acidified by addition of 0.02 M CF_3COOH showed an identical spectrum. Further, photolysis of 20% *(v/v)* di-*t*-butyl peroxide in toluene which is known to yield benzyl radicals lead to the same spectrum in the accessible spectral range of $\lambda \geqq 300$ nm. The absorption spectrum of benzyl has first been reported by *Porter & Wright* [18] in the gas-phase and later by many authors [19] under various conditions. In agreement with the literature we find a strong transition at $\lambda = 258$ nm, a band system of weaker intensity with a maximum at $\lambda = 316$ nm, and a very weak long wavelength band system with a maximum at 452 nm. The latter system has previously been observed in absorption [20] [21] and emission [22] [23]. As a closer comparison with published spectra reveals our spectrum is practically undistorted

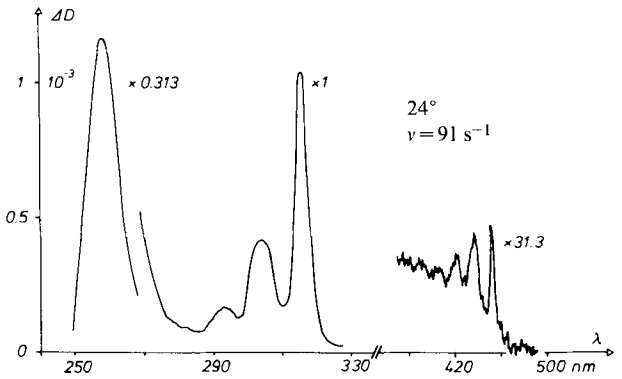

Fig. 13. *Absorption spectrum of benzyl radicals in cyclohexane*

by radical-substrate interactions [19], and contributions of products causing a shoulder at 324 nm [22] or a permanent absorption at 258 nm [20]. The lifetime τ_R and $\varepsilon_R \cdot I_0$ for benzyl were determined as before from the frequency dependencies of ΔD and φ. Solutions of 0.00146 and 0.00179 M ketone in cyclohexane were applied at room temperature. The rate of radical formation I_0 was measured from the decay of the radical signal after interrupt of the flow at a high modulation frequency.

It was found impossible to apply the alternative procedure of obtaining I_0 from the effect spectrum at low modulation frequencies in this case, since there were distortions of the $n\pi^*$-transition of the ketone by unknown minor reaction products. The extinction coefficients ε_R of benzyl and the termination rate constant k resulting from I_0, $\varepsilon_R I_0$ and τ_R are listed in the *Table*. For $\lambda = 316$ nm we find $\varepsilon_R = (8800 \pm 700)$ M^{-1} cm^{-1}. In general, this value agrees well with literature data. For instance, in cyclohexane solvent $\varepsilon_R = 12{,}000$ M^{-1} cm^{-1} [24] and $\varepsilon_R = 9000$ M^{-1} cm^{-1} [19] have been reported. For water as solvent, $\varepsilon_R = 9000$ [20], 8520 [25], 5500 [21d] and 2000 M^{-1} cm^{-1} [26] were found, and in alcohols the values of $\varepsilon_R = 2000$ [26] and 1100 M^{-1} cm^{-1} [27] were determined. Less well comparable are the low-temperature data obtained from glasses ($\varepsilon_R = 19{,}000$ [28], 18,000 [29] and 12,000 [29]) and the very large gase-phase result of $\varepsilon_R \leqq 10^6$ M^{-1} cm^{-1} [30].

5. Discussion. – The main results, *i.e.* the principal spectral features and the self-termination rate constants of the radicals, are collected in the *Table* where the standard deviations of the data are also given. In the last column ratios of the experimental to theoretical rate constants are listed. The theoretical values were obtained in the following way: As before (see [1]) we assume that the self-termination of small sterically unhindered radicals is diffusion controlled and well described by the *von Smoluchowski*-equation

$$2k^{th} = \frac{8\pi}{1000} \cdot N_L \cdot \sigma \cdot \rho \cdot D \tag{35}$$

where D is the diffusion coefficient of the radicals in the solvent, ρ the reaction distance and $\sigma = 1/4$ a spin statistical factor. Further, we approximate D by the diffusion coefficient of stable hydrocarbon analogs (isobutane for *t*-butyl, propane for 2-propyl, toluene for benzyl) and ρ by the molecular diameter of these compounds. For this work we measured the diffusion coefficients by a method described previously [1d] and found $D = 3.62 \cdot 10^{-6}$ cm^2 s^{-1} for isobutane in 3-methyl-3-pentanol at 10°, $D = 1.54 \cdot 10^{-5}$ cm^2 s^{-1} for propane in hexadecane at 39° and used $D = 1.58 \cdot 10^{-5}$ cm^2 s^{-1} for toluene in cyclohexane at room temperature. The reaction diameters of $\rho = 5.63$ Å for *t*-butyl [1b], $\rho = 5.80$ Å for benzyl [1c] and $\rho = 5.22$ Å for 2-propyl were applied, the latter value was estimated by the methods given in [1c]. As the *Table* clearly reveals, the experimental and the theoretical rate constants agree within the experimental error limits. This reinforces our previous conclusions on the factors controlling the rates of self-termination of transient free radicals in solution [1]. Finally, it may be mentioned that the absolute

rate constants obtained here *via* optical spectroscopy agree well with our previous results derived by kinetic ESR. spectroscopy and confirm the inherent accuracy of both methods.

Support by the *Swiss National Science Foundation* is gratefully acknowledged.

REFERENCES

[1] a) *H. Schuh & H. Fischer,* Int. J. Chem. Kinet. *8*, 341 (1976); b) *H. Schuh & H. Fischer,* Helv. *61*, 2130 (1978); c) *M. Lehni, H. Schuh & H. Fischer,* Int. J. Chem. Kinet. *11*, 705 (1979); d) *C. Huggenberger, J. Lipscher & H. Fischer,* J. Phys. Chem., submitted, and references therein.

[2] a) *L.M. Dorfman & M.S. Matheson,* Progr. Reaction Kinet. *3*, 237 (1965); b) *P. Neta,* Adv. Phys. Org. Chem. *12*, 223 (1976).

[3] a) *E.J. Land,* Progr. Reaction Kinet. *3*, 369 (1965); b) *F.W. Willets,* ibid. *6*, 51 (1971).

[4] *H. Labhart & W. Heinzelmann, in* 'Organic Molecular Photolysis', ed. J.B. Birks, Wiley, New York 1973, Vol. I, p. 297ff.

[5] a) *H.E. Hunziker,* IBM J. Res. Dev. *15*, 10 (1971); b) *H.E. Hunziker & H.R. Wendt,* J. Chem. Phys. *64*, 3488 (1976).

[6] *F. Graf, K. Loth, M. Rudin, M. Forster, T.-K. Ha & Hs.H. Günthard,* Chem. Phys. *23*, 327 (1977) and references cited therein.

[7] *H. Paul,* J. Chem. Phys. *15*, 115 (1976), Int. J. Chem. Kinetics *11*, 495 (1979) and references cited therein.

[8] *T.T. Paukert & H.S. Johnston,* J. Chem. Phys. *56*, 2824 (1972).

[9] a) *D.A. Parkes, D.M. Paul & C.P. Quinn,* J. Chem. Soc. Faraday Trans. I *72*, 1935 (1976); b) *D.A. Parkes & C.P. Quinn,* Chem. Phys. Lett. *33*, 483 (1975); c) J. Chem. Soc. Faraday Trans. I *72*, 1952 (1976).

[10] *J. Yguerabide,* Rev. Scient. Instr. *39*, 1048 (1968).

[11] *N.C. Yang, E.D. Feit, M.M. Hui, N.J. Turro & J.C. Dalton,* J. Am. Chem. Soc. *92*, 6974 (1970).

[12] a) *H. Schuh, E.J. Hamilton, Jr., H. Paul & H. Fischer,* Helv. *57*, 2011 (1974); b) *H. Schuh & H. Fischer,* ibid. *61*, 2463 (1978).

[13] *H. Paul & H. Fischer,* Helv. *56*, 1575 (1973).

[14] *S.G. Whiteway & C.R. Masson,* J. Am. Chem. Soc. *77*, 1508 (1955).

[15] *J. Lipscher & H. Fischer,* to be published.

[16] *P. Arrowsmith & L.J. Kirsch,* J. Chem. Soc. Faraday Trans. I *74*, 3016 (1978).

[17] *H. Langhals & H. Fischer,* Chem. Ber. *111*, 543 (1978), and references cited therein.

[18] *G. Porter & F.J. Wright,* Trans. Faraday Soc. *51*, 1469 (1955).

[19] *N.A. McAskill & D.F. Sangster,* Aust. J. Chem. *30*, 2107 (1977) and references therein.

[20] *J.P. Mittal & E. Hayon,* Nature *240*, 20 (1972).

[21] a) *G. Porter & E. Strachan,* Spectrochim. Acta *12*, 299 (1958); b) *G. Porter & B. Ward,* J. Chim. Phys. *61*, 1517 (1964); c) *W.H. Hamill, J.P. Guarino, M.R. Ronayne & J.A. Ward,* Discuss. Faraday Soc. *36*, 169 (1963); d) *H.C. Christensen, K. Sehested & E.J. Hart,* J. Phys. Chem. *77*, 983 (1973).

[22] *E.J. Jordan, D.W. Pratt & D.E. Wood,* J. Am. Chem. Soc. *96*, 5588 (1974).

[23] a) *H. Schuler & M. Stockburger,* Spectrochim. Acta *13*, 841 (1959); b) *P.M. Johnson & A.C. Albrecht,* J. Chem. Phys. *48*, 851 (1968).

[24] *R.J. Hagemann & H.A. Schwarz,* J. Phys. Chem. *71*, 2694 (1967).

[25] *M.Z. Hoffmann & E. Hayon,* J. Phys. Chem. *77*, 990 (1973).

[26] *T.O. Meiggs, L.I. Grossweiner & S.I. Miller,* J. Am. Chem. Soc. *94*, 7981, 7986 (1972).

[27] *R.L. McCarthy & A. MacLachlan,* Trans. Faraday Soc. *56*, 1187 (1960).

[28] *J.E. Hodgkins & E.D. Megarity,* J. Am. Chem. Soc. *87*, 5322 (1965).

[29] *J.B. Giallivan & W.H. Hamill,* Trans. Faraday Soc. *61*, 1960 (1965).

[30] *F. Bayrakceken & J.E. Nicholas,* J. Chem. Soc. London B *1970*, 691.